THE EFFECT OF POROSITY ON THE STRUCTURE AND PROPERTIES OF CALCIUM POLYPHOSPHATE BIOCERAMICS

QIANBIN WANG, QIGUANG WANG*, CHANGXIU WAN*

School of Chemistry and Environment, Beihang University, Beijing 100191, P. R. China
**College of Polymer Science and Engineering, Sichuan University, Chengdu 610065, P. R. China*

E-mail: wanchx@scu.edu.cn

Submitted June 12, 2010; accepted March 27, 2011

Keywords: calcium polyphosphate, Porosity, Microstructure, Degradability, Compressive strength

Calcium polyphosphate (CPP) bioceramic with different porosities were prepared by controlling the concentration of the pore-foaming agent. Effect of porosity (0%, 15%, 30%, 45% and 60%) on the microstructure, pores interconnection, dissolution behavior and compressive strength of CPP bioceramic were investigated. Scanning electron microscope (SEM) and capillarity test results indicated that CPP with higher porosity (45% and 60%) exhibited three-dimensional interconnected pore structure with a pore size of about 200–400 μm, while the pores of lower porosity scaffold (0%, 15% and 30%) were isolated. The dissolution behavior in vitro indicated that the dissolution rate accelerated with the porosity increasing and the CPP with 60% porosity showed the highest dissolution velocity. The compressive strength of porosity CPP scaffolds were as much as the human cancellous bone, which decreased with the increase of porosity. While the dense CPP scaffolds lie in the same order of magnitude as compact bone.

INTRODUCTION

The development of bone tissue engineering depends partly but strongly upon the scaffolds [1]. A scaffold is considered to be a temporary platform that provides structural support to the regenerating region but degrades concurrent with tissue formation [2]. In general, an ideal scaffold should have several characteristics: (i) high porosity for cell/tissue growth, nutrient diffusion, matrix production and vascularization; (ii) controllable degradation to match tissue growth once implanted in a body and (iii) reasonable mechanical strength to match the tissues at the site of implantation [3].

Nowadays, several kinds of artificial bone implant materials were widely used, such as hydroxyapatite (HA), tricalcium phosphate (TCP) and bioglass. However, the research of Hench LL [4] demonstrated that the dissolution velocity of HA was generally slow while β-TCP relatively fast, both of which were incompatible with bone regeneration. To overcome their disadvantages, some glasses and glass-ceramics have been developed, such as Bioglasss®, Bioverits® and Ceravitals®. Nevertheless, all these materials still lack both osteogenic properties and complete biodegradability after implantation [4]. Calcium polyphosphate (CPP), a new promising biomaterial for bone tissue engineering, has been fast development since it was rediscovery and use in bone regeneration [5-8]. CPP has drawn many researchers' attention not only for it's outstanding biocompatibility [9-10] but also for the controllable degradability [11-13], excellent compressive strength, similar chemical elements with bones and diversity in chemical composition [14, 15]. Previous studies by Ding and Qiu [11, 16] exploring the effect of the polymerization degree on the mechanical performance and degradation behavior of CPP showed that with the increase of the polymerization degree, the compressive strength was promoted and the degradability was weaken. From evaluating the in vivo behavior of porous CPP samples, Pilliar et al. [5-8] suggested its potential as a bone substitute. All of these studies indicated that CPP was an ideal bioceramic with excellent osteoinduction and osteoconduction for bone substitute.

The aim of the present work was to study the effect of porosity on the microstructure and properties of calcium polyphosphate. The pore size and pore structure of the samples were assessed in terms of SEM pattern. Capillarity test was used to investigate the pores interconnection of scaffold. In addition, the effect of porosity on the immersion behavior and compressive strength were also investigated.

EXPERIMENTAL

CPP scaffolds with different porosities were prepared as previously described [17]. Briefly, calcium carbonate was added slowly into the phosphoric acid (85 %) with stirring respectively. After the reaction went on at room temperature overnight, the solution was evaporated in vacuum. The precipitates were collected and washed by ethanol (95%) until the pH of filtrate was about 7. Then the powders were calcined to form CPP. After screened to yield powders in a size range of <75 μm, the amorphous powders were mixed with different amount of stearic acid to fabricate porous CPP scaffolds with different porosities by sintering.

Microstructure study was carried out by scanning electron microscopy (JSM-5900LV, Japan). A liquid displacement method was used to measure the porosity of scaffolds [18]. Ethanol was used as a liquid medium. The porosity was expressed as:

$$\text{Porosity} = \frac{W_2 - W_1}{W_2 - W_3} \times 100\ \% \qquad (1)$$

where W_1 is the weight of sample in air, W_2 the weight of sample with liquid in pores, and W_3 the weight of sample suspended in ethanol. The interconnection of the pore was qualitatively assessed by means of capillarity test. A face of the scaffold was put into contact with a viscous solution (30 wt.% of calf serum and 70 wt. % of distilled water [19]). In order to better observe the capillarity uptake of the fluid, red ink was dropped into the solution.

The degradation testing was performed in Tris-HCl buffer solution (pH = 7.4) at 37 ± 0.5°C with a continual agitation speed of 120 rpm according to ISO 10993-14. At the end of each immersion time, distilled water was used to wash the sample surface, and then samples were dried until a constant weight. By using a colorimetric method, orthophosphate ion concentration in degraded medium was measured [20]. Calcein titration method was used to measure the Ca^{2+} concentration change in degraded solution [21]. Weight loss for each sample during degradation was measured by equation as follow:

$$\text{Weightloss} = \frac{W_0 - W_t}{W_0} \times 100\ \% \qquad (2)$$

where W_0 and Wt stand for initial weight and weight after a specific immersion time, respectively. Moreover, the pH value was also measured. Each measured sample contains three parallel test samples.

Table 1. Samples used in this paper and the porosity of CPP measured by liquid displacement method.

Samples	Theoretical porosity	Measurement porosity
CPP0	0 %	(14.2 ±1.0) %
CPP15	15 %	(25.2 ±1.2) %
CPP30	30 %	(46.4 ±1.2)%
CPP45	45 %	(63.2 ±1.7) %
CPP60	60 %	(78.5 ±1.6) %

Compression test was conducted with an Instron 4302 material testing system (American). The crosshead speed was set at 1 mm/min, and the load was applied until the scaffold was cracked.

RESULTS AND DISCUSSION

Figure 1 is the XRD pattern of CPP prepared by gravity sintering. The three characteristic peaks between 20~30° indicated the crystalline structure was considered to be β-CPP. Figure 2 shows SEM photographs of CPP with different porosities, respectively. It is viewed that the diameter of the pores are all about 200-400 μm and the samples show different porosities. CPP45 and CPP60 (Table 1) exhibit three-dimensionally interconnected pore structure, while the pores of CPP0, CPP15 and CPP30 are isolated. As expected, most of the spherical pores obtained in the high porosity scaffold are connected to the neighboring pores through throats. It has been demonstrated that well bone tissue engineering scaffolds should exhibit pore content and size according to the type and need of the specific cells. Pores above 100 μm (big pores) allow the scaffold colonization by osteoblasts, while the micro-pores (≤ 50 μm) promote scaffold vascularization (nutrients supplying for cells, waste products removal) [22]. There are many little pores around the big pores shown in Figure 2, which indicated that multiscale pores are obtained successfully.

In this paper, CPP scaffolds with different porosities were prepared by using different stearic acid amounts in the range 0-60 wt%. Table 1 groups the values of porosity measured by liquid displacement method, which allows characterization of the open porosity. As expected, the porosity of the scaffold increased with the increase of porogen. It was noted that the actual porosity is higher than the theoretical one (percent of the pore-foaming agent), which indicated that sintering procedure would cause some little pores as shown in the SEM patterns (Figure 2).

The sequence of photographs shown in Figure 3 depicts the phases of the capillarity test performed on CPP scaffold. The calf serum went up through scaffold

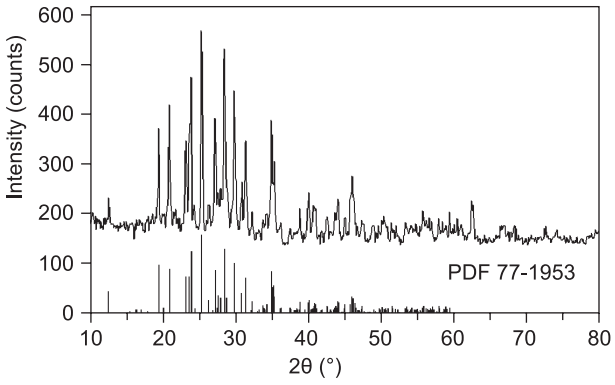

Figure 1. XRD pattern of CPP prepared by gravity sintering.

pores network in a couple of seconds. Figure 3 reports the result of capillarity tests on CPP45: the fluid went up through scaffold pore network in ~4.9s, thus further confirmed the high interconnection degree of this porous structure. Similar results were obtained for CPP0, CPP15, CPP30 and CPP60. The times of CPP15, CPP30 and CPP60 are ~36.1, ~10.0 and ~2.5s, respectively, while the fluid can not go up through the CPP0 scaffold. The capillarity was obvious for the scaffold with highly interconnected porosity.

Porosity and pore size of scaffolds play a critical role in bone formation *in vitro* and *in vivo*. The most porous structures are more likely to offer good conditions for cell growth and flow transrt of nutrients and metabolic waste, because of their higher specific surface area, while the dense scaffold may provide excellent mechanical strength when implanted in body. Similarly, the pore size can affect the cell attachment, proliferation and flow transport of nutrients and metabolic waste. For bone tissue engineering, the optimal pore size required for bone ingrowth has been suggested in the range of 100–800 μm [23].

The effect of different porosities of CPP after soaking in Tris-HCl buffer solution for 60 hours on their weight loss is showed in Figure 4, respectively. The weight loss showed a steady increase with the increase of the immersion period, which presented a similar trend for all scaffolds. Scaffolds with different porosities showed different dissolution rate. With the porosity increasing from 0% to 60%, the dissolution rate of CPP accelerated.

As shown in Figure 5, the ion concentration of the testing solution increased with increase of the soaking time, which supports the relative weight loss values presented in Figure 4. And all samples presented a similar trend, with a steady increase in ion concentration as the immersion period increasing. CPP60 showed the highest dissolution rate in all samples, which lose PO_4^{3-} concentration of 552 mg/L in 60 hours degradation in Tris-HCl buffer solution. In contrast, within the same time PO_4^{3-} concentration loss of CPP0 were 185 mg/L.

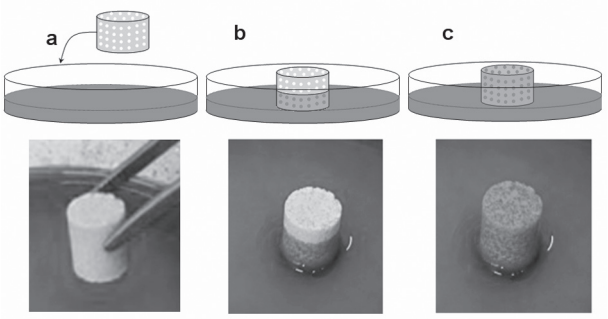

Figure 3. Capillarity test (a-c) phases of the test carried out on CPP45 scaffold.

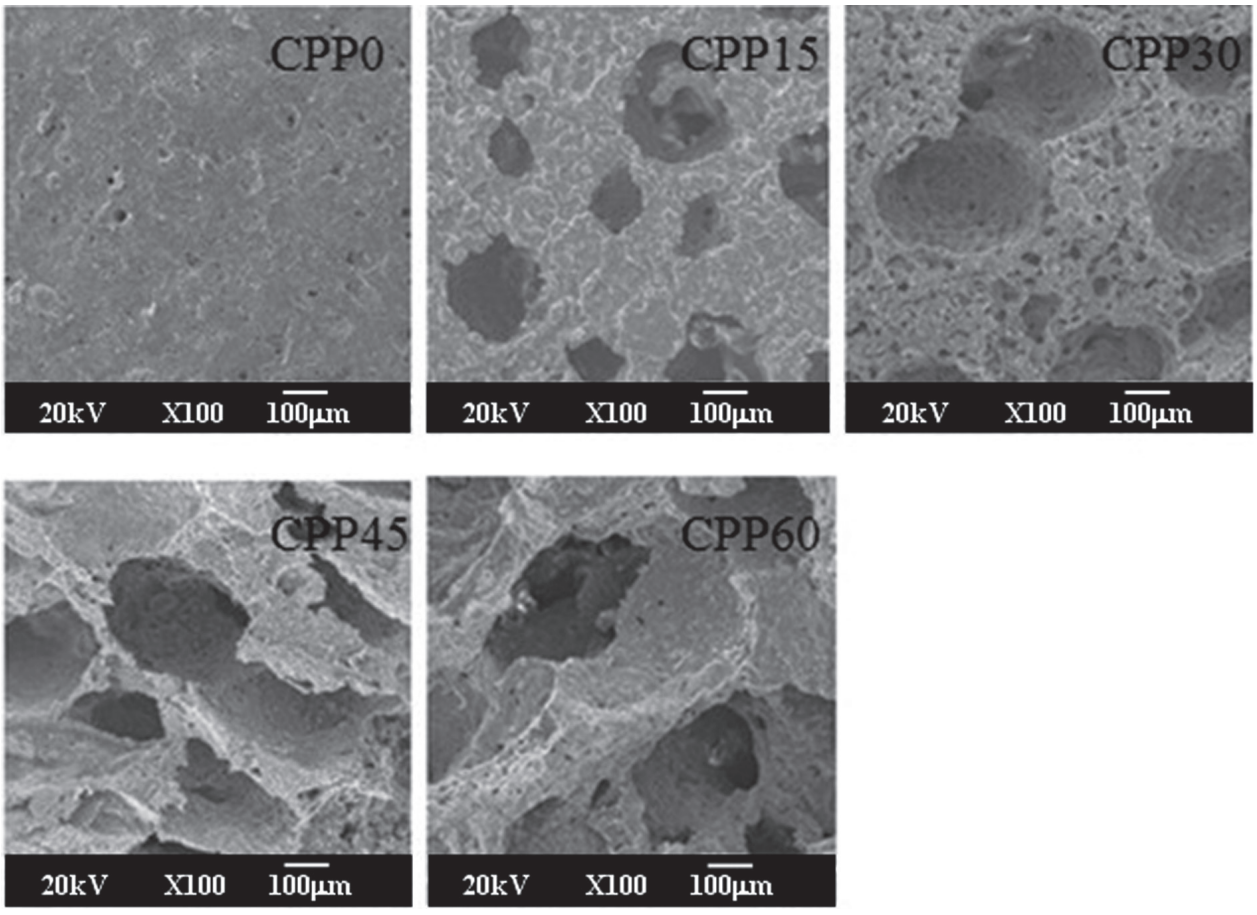

Figure 2. SEM pictures of calcium polyphosphate with different porosities.

Figure 6 depicted the variation of pH with immersion time. It was observed a significant decrease in the pH of all samples. The pH was decreased from 7.4 to approximately 6.6 after 60 hours of immersion in Tris-HCl buffer solution.

Changing the textural porosity of the scaffolds had an effect on the dissolution behavior of the scaffolds (Figure 4 and Figure 5) due to changes in the specific surface area of sample exposed to the degradation media. When the CPP samples were put into the degradation solution, the liquid contacted with the sample surface first, that is the formation of materials-liquid interface. Then the fluid went up through the interconnection pore by capillarity, here the pore walls became new materials-liquid interface. The increased porosity resulted in a higher surface area, which eventually caused the higher dissolution rate.

The compressive strength values of CPP scaffolds with different porosities are presented in Figure 7. The mechanical behavior of CPP shows an inverse relationship with porosity. They range from 2.3 MPa for the most porous sample, 78.5% porosity (CPP60), to 168 MPa for the least porous sample, 14.2% porosity (CPP0). Table 2 presents values given in the literatures for bone compressive strength for comparison. In general, cancellous bone has a compressive strength in the range of 1 to 100 MPa, and compact bone has a compressive strength of 130 to 200 MPa [24, 25]. As can be seen, CPP0 lie in the same order of magnitude of compact bone. While the porous specimens (25.2% to 78.5%) range from 79.8 MPa to 2.3 MPa, so they lie in the rigidity value interval reported by Gibson et al. [24] for human cancellous bone: between 1 to 100 MPa.

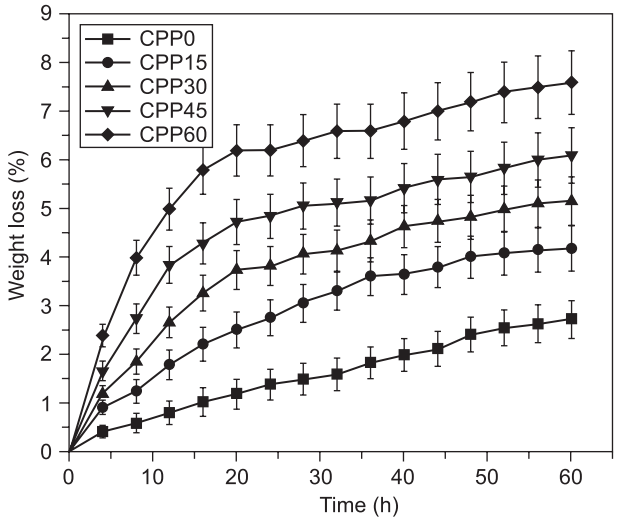

Figure 4. Weight loss of calcium polyphosphate in Tris-HCl buffer solution.

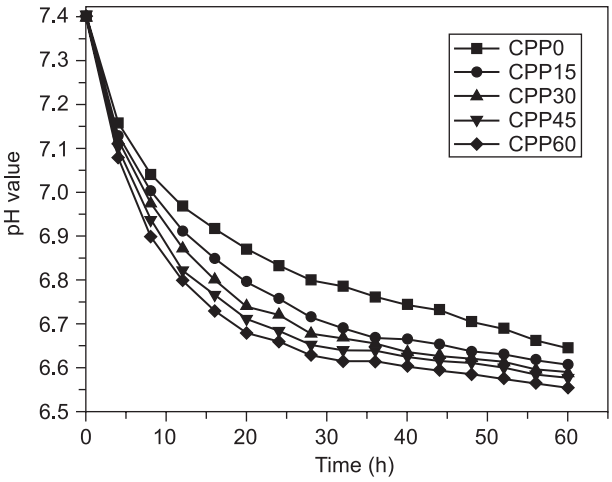

Figure 6. pH change of calcium polyphosphate in Tris-HCl buffer solution.

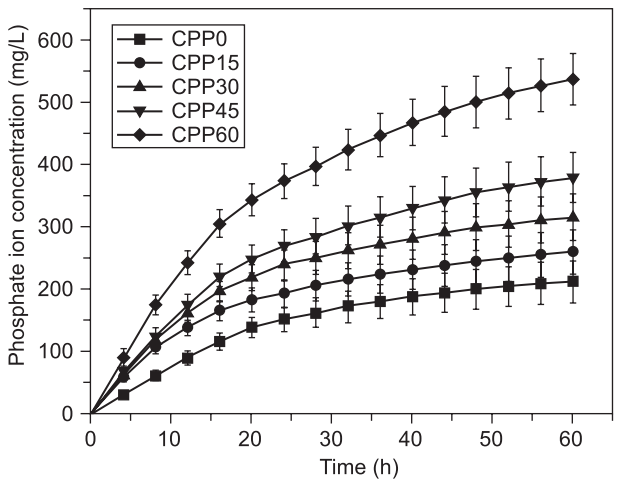

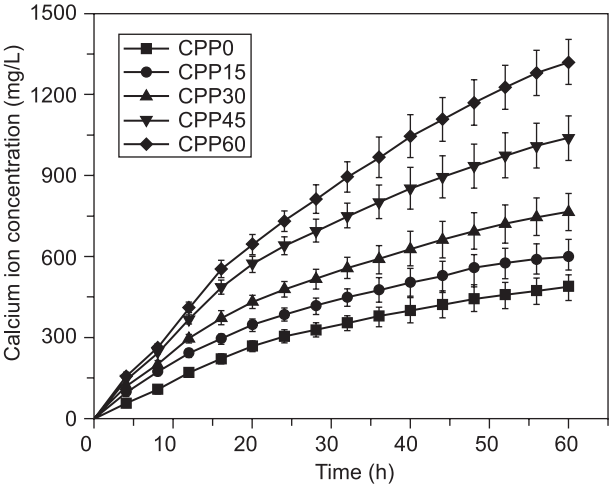

Figure 5. The phosphate ion (a) and calcium ion (b) concentration in the degradation media.

Table 2. Mean values for bone ultimate strength.

Type of bone	Direction andtype of load	Ultimate strengh (MPa)	Reference
Cortical (midfemoral)	Longitudinal compression	193	[27]
	Transverse compression	33	[27]
Trabecular (proximal tibia)	Axial	5.3	[28]
Trabecular (proximal femoral)		6.8	[29]
Compact bone		130-200	[24]
Cancellous bone		1-100	[25]

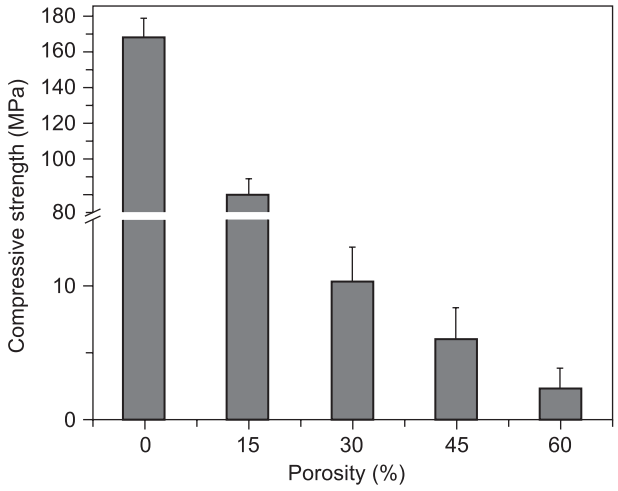

Figure 7. Compressive strength of calcium polyphosphate scaffold with different porosities.

Biomechanics is one important function of bone. So the design of scaffold for bone tissue engineering must have reasonable mechanical strength. In general, the scaffold would provide a stable mechanical environment similar to the natural bone. Compared with the mechanical strength of human bone, it is confirmed that CPP could be an interesting candidate biomaterial for bone implant, at least on the mechanical point of view.

CONCLUSION

Our findings demonstrated that the high porosity CPP exhibited three-dimensional interconnected pore structure, fine pore size, controllable degradability and reasonable compressive strength, which suggested that the porous CPP may be an ideal scaffold for bone tissue engineering. While the dense CPP was biodegradable and showed excellent compressive strength much as human compact bone, which suggested that it may be an ideal bioceramic for loaded bone implant. These findings may also provide an approach to achieve a fine microstructure, controllable degradability and high strength scaffold and explore more biomedical applications.

Acknowledgment

The authors are grateful to the NSFC for providing financial support through project 30870614. The author would also like to thank the professors in the Centre of Analysis and Testing of Sichuan University who provided the SEM measurement.

References

1. Agrawal C. M., Ray R. B.: J Biomed Mater Res *55*, 141 (2001).
2. Drury J. L., Mooney D. J.: Biomaterials *24*, 4337 (2003).
3. Hutmacher D. W.: Biomaterials *21*, 2529 (2000).
4. Hench L. L.: Journal of the American Ceramic Society *81*, 1705 (1998).
5. Pilliar R. M., Filiaggi M. J., Wells J. D., Grynpas M. D., Kandel R. A.: Biomaterials *22*, 963 (2001).
6. Grynpas M. D., Pilliar R. M., Kandel R. A., Renlund R., Filiaggi M., Dumitriu M.: Biomaterials *23*, 2063 (2002).
7. El Sayegh T. Y., Pilliar R. M., McCulloch C. A. G.: Journal of Biomedical Materials Research *61*, 482 (2002).
8. Waldman S. D., Grynpas M. D., Pilliar R. M., Kandel R. A.: Journal of Biomedical Materials Research *62*, 323 (2002).
9. Park E. K.; Lee Y. E., Choi J. Y., Oh S. H., Shin H. I., Kim K. H.: Kim S. Y., Kim S.: Biomaterials *25*, 3403 (2004).
10. Yang S. M., Kim S. Y., Lee S. J., Lee Y. K., Lee Y. M., Ku Y., Chung C. P., Han S. B., Rhyu I. C.: Key Engineering Materials *254*, 245 (2004).
11. Ding Y. L., Chen Y. W., Qin Y. J., Shi G. Q., Yu, X. X., Wan C. X.: Journal of Materials Science-Materials in Medicine *19*, 1291 (2008).
12. Wang Q. B., Wang Q. G., Zhang X. H., Yu X. X., Wan C. X.: *Ceramics - Silikaty 54,* 97 (2010).
13. Wang Q. B., Wang Q. G., Wang J. Y., Zhang X. H., Yu X. X., Wan C. X.: Materials Research *12*, 495 (2009).
14. Dias A. G., Lopes M. A., Gibson I. R., Santos, J. D.: Journal of Non-Crystalline Solids *330*, 81 (2003).
15. Gomez F., Vast P., Llewellyn P., Rouquerol F.: Journal of Non-Crystalline Solids *222*, 415 (1997).
16. Qiu K., Wan C. X., Chen X., Zhang Q., Su H. F.: Key Engineering Materials *288*, 553 (2005).
17. Qiu K., Zhao X. J., Wan C. X., Zhao C. S., Chen Y. W.: Biomaterials *27*, 1277 (2006).
18. Li X., Li D. C., Lu B. H., Wang C. T.: Journal of Porous Materials *15*, 667 (2008).

19. Vitale-Brovarone C., Miola M., Balagna C., Verné E.: Chemical Engineering Journal *137*, 129 (2007).
20. Fiske C. H., Subbarow Y. C. H., Fiske, Subbarow Y.: Journal of Biological Chemistry *66*, 375 (1925).
21. Dion A., Langman M., Hall G., Filiaggi M.: Biomaterials *26*, 7276 (2005).
22. Kieswetter K., Schwartz Z., Hummert T., Cochran D., Simpson J., Dean D., Boyan B.: Journal of Biomedical Materials Research Part A *32*, 55 (1996).
23. Sous M, Bareille R, Rouais F, et al. Biomaterials. 1998;19:2147–53.
24. Gibson, L. J.: Journal of Biomechanics *18*, 317 (1985).
25. Reilly, D. T., Burstein, A. H.: Journal of Biomechanics *8*, 393 (1975).
26. Lanza R. P., Langer R., Vacanti J.: Principles of Tissue Engineering, Academic Press, San Diego, (2000).
27. Cullinane D. M., Einhorn T. A.: Biomechanics of bone, Avademic Press, San Diego, (2002).
28. Linde F, Hvid I.: Journal of Biomechanics *22*, 485 (1989).
29. Rohlmann A, Zilch H, Bergmann G, Kolbel R.: Archives of Orthopaedic and Trauma Surgery *97*, 95 (1980).